

**This is a self-archived version of an original article. This version may differ from the original in pagination and typographic details.**

**Author(s):** Auranen, K.; Seweryniak, D.; Albers, M.; Ayangeakaa, A.D.; Bottoni, S.; Carpenter, M.P.; Chiara, C.J.; Copp, P.; David, H.M.; Doherty, D.T.; Harker, J.; Hoffman, C.R.; Janssens, R.V.F.; Khoo, T.L.; Kuvin, S.A.; Lauritsen, T.; Lotay, G.; Rogers, A.M.; Scholey, Catherine; Sethi, J.; Talwar, R.; Walters, W.B.; Woods, P.J.; Zhu, S.

**Title:** Proton decay of  $108\text{l}$  and its significance for the termination of the astrophysical rp-process

**Year:** 2019

**Version:** Published version

**Copyright:** © 2019 Published by Elsevier B.V.

**Rights:** CC BY 4.0

**Rights url:** <https://creativecommons.org/licenses/by/4.0/>

**Please cite the original version:**

Auranen, K., Seweryniak, D., Albers, M., Ayangeakaa, A.D., Bottoni, S., Carpenter, M.P., Chiara, C.J., Copp, P., David, H.M., Doherty, D.T., Harker, J., Hoffman, C.R., Janssens, R.V.F., Khoo, T.L., Kuvin, S.A., Lauritsen, T., Lotay, G., Rogers, A.M., Scholey, C., . . . Zhu, S. (2019). Proton decay of  $108\text{l}$  and its significance for the termination of the astrophysical rp-process. *Physics Letters B*, 792, 187-192. <https://doi.org/10.1016/j.physletb.2019.03.039>



# Proton decay of $^{108}\text{I}$ and its significance for the termination of the astrophysical $rp$ -process

K. Auranen<sup>a,\*</sup>, D. Seweryniak<sup>a</sup>, M. Albers<sup>a</sup>, A.D. Ayangeakaa<sup>a,1</sup>, S. Bottoni<sup>a,2</sup>, M.P. Carpenter<sup>a</sup>, C.J. Chiara<sup>a,b,3</sup>, P. Copp<sup>a,c</sup>, H.M. David<sup>a,4</sup>, D.T. Doherty<sup>d,5</sup>, J. Harker<sup>a,b</sup>, C.R. Hoffman<sup>a</sup>, R.V.F. Janssens<sup>e,f</sup>, T.L. Khoo<sup>a</sup>, S.A. Kuvin<sup>a,g</sup>, T. Lauritsen<sup>a</sup>, G. Lotay<sup>h</sup>, A.M. Rogers<sup>a,6</sup>, C. Scholey<sup>i,7</sup>, J. Sethi<sup>a,b</sup>, R. Talwar<sup>a</sup>, W.B. Walters<sup>b</sup>, P.J. Woods<sup>d</sup>, S. Zhu<sup>a</sup>

<sup>a</sup> Physics Division, Argonne National Laboratory, 9700 South Cass Avenue, Lemont, IL 60439, USA

<sup>b</sup> Department of Chemistry and Biochemistry, University of Maryland, College Park, MD 20742, USA

<sup>c</sup> Department of Physics and Applied Physics, University of Massachusetts Lowell, Lowell, MA 01854, USA

<sup>d</sup> University of Edinburgh, Edinburgh EH9 3JZ, United Kingdom

<sup>e</sup> Department of Physics and Astronomy, University of North Carolina at Chapel Hill, Chapel Hill, NC 27599, USA

<sup>f</sup> Triangle Universities Nuclear Laboratory, Duke University, Durham, NC 27708, USA

<sup>g</sup> Department of Physics, University of Connecticut, Storrs, CT 06269, USA

<sup>h</sup> University of Surrey, Guildford GU2 7XH, United Kingdom

<sup>i</sup> Department of Physics, University of Jyväskylä, P.O. Box 35, FI-40014 University of Jyväskylä, Finland

## ARTICLE INFO

### Article history:

Received 8 February 2019

Received in revised form 12 March 2019

Accepted 20 March 2019

Available online 22 March 2019

Editor: D.F. Geesaman

### Keywords:

$\alpha$  decay

Proton decay

Astrophysical  $rp$  process

$^{104}\text{Sb}$

$^{107}\text{Te}$

$^{108}\text{I}$

## ABSTRACT

Employing the Argonne Fragment Mass Analyzer and the implantation-decay-decay correlation technique, a weak 0.50(21)% proton decay branch was identified in  $^{108}\text{I}$  for the first time. The  $^{108}\text{I}$  proton-decay width is consistent with a hindered  $l = 2$  emission, suggesting a  $ds_{1/2}$  origin. Using the extracted  $^{108}\text{I}$  proton-decay  $Q$  value of 597(13) keV, and the  $Q_\alpha$  values of the  $^{108}\text{I}$  and  $^{107}\text{Te}$  isotopes, a proton-decay  $Q$  value of 510(20) keV for  $^{104}\text{Sb}$  was deduced. Similarly to the  $^{112,113}\text{Cs}$  proton-emitter pair, the  $Q_p(^{108}\text{I})$  value is lower than that for the less-exotic neighbor  $^{109}\text{I}$ , possibly due to enhanced proton-neutron interactions in  $N \approx Z$  nuclei. In contrast, the present  $Q_p(^{104}\text{Sb})$  is higher than that of  $^{105}\text{Sb}$ , suggesting a weaker interaction energy. For the present  $Q_p(^{104}\text{Sb})$  value, network calculations with the one-zone X-ray burst model Mazzocchi et al. (2007) [18] predict no significant branching into the Sn-Sb-Te cycle at  $^{103}\text{Sn}$ .

© 2019 Published by Elsevier B.V. This is an open access article under the CC BY license (<http://creativecommons.org/licenses/by/4.0/>). Funded by SCOAP<sup>3</sup>.

## 1. Introduction

Nuclear structure and binding energies of exotic, neutron-deficient nuclei can be extracted from their  $\alpha$ - and proton-decay properties. Far from the valley of  $\beta$  stability, where experiments are particularly challenging, due to low production cross sections, this is often the only method available. The region in the vicinity of the  $N = Z$  line, close to  $^{100}\text{Sn}$  [1], is a prime example of such nuclei, which are of special interest as they are close to the  $N = Z = 50$  double shell closure. They are known to exhibit exotic nuclear phenomena, such as the largest Gamow–Teller  $\beta$ -decay strength [2], superallowed  $\alpha$  decay [3–8], as well as possible cluster [9–11] and two-proton emission [12–14]. Some of the nuclei “northeast” of  $^{100}\text{Sn}$  spontaneously emit protons. In fact,  $^{109}\text{I}$  and  $^{113}\text{Cs}$  were the first two proton emitters where inclusion of deformation was needed to calculate their proton-decay half-lives

\* Corresponding author.

E-mail address: [kauranen@anl.gov](mailto:kauranen@anl.gov) (K. Auranen).

<sup>1</sup> Present address: Department of Physics, United States Naval Academy, Annapolis, Maryland 21402, USA.

<sup>2</sup> Present address: Università degli Studi di Milano and INFN, Via Celoria 16, I-20133 Milano, Italy.

<sup>3</sup> Present address: U.S. Army Research Laboratory, Adelphi, Maryland 20783, USA.

<sup>4</sup> Present address: GSI, Planckstraße 1, D-64291, Darmstadt, Germany.

<sup>5</sup> Present address: University of Surrey, Guildford GU2 7XH, United Kingdom.

<sup>6</sup> Present address: Department of Physics and Applied Physics, University of Massachusetts Lowell, Lowell, Massachusetts 01854, USA.

<sup>7</sup> Present address: MTC Limited, Ansty Park, Coventry CV7 9JU, UK.

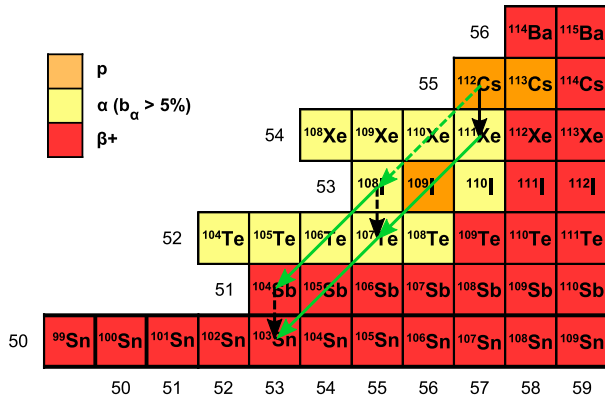


**Fig. 1.** The nuclear chart in the proximity of  $^{100}\text{Sn}$ . A nucleus is marked as an  $\alpha$  emitter, if it has an  $\alpha$ -decay branch greater than 5%. The proton and  $\alpha$  decays relevant for this work are indicated with black and green arrows, respectively. Decays observed in earlier experiments are indicated with solid lines, whereas those studied in this work are marked with dashed lines.

[15,16]. Recently, state-of-the-art nonadiabatic quasiparticle model of proton decay [17] required addition of triaxiality to reproduce the measured  $^{109}\text{I}$  proton-decay rate [18]. Interestingly, the protons in the odd-odd  $^{112}\text{Cs}$  are more bound than in  $^{113}\text{Cs}$ , resulting in longer half-life for the more exotic nucleus [19]. Similar half-life anomaly was recently reported for the lighter  $N \approx Z$  nuclei  $^{72,73}\text{Rb}$  [20]. In addition, odd-odd proton emitters shed light on the role of the odd neutron, which does not participate in the proton decay, but it determines the spin of the proton-decaying state and thus influences the proton-decay rate [21].

Antimony isotopes act as a gate for the astrophysical  $rp$ -process flow towards the region of  $\alpha$  activity, starting with the tellurium isotopes. Proton separation energies ( $S_p = -Q_p$ ) of antimony isotopes determine the breakout path. It has been suggested that the  $rp$ -process terminates in a Sn-Sb-Te cycle, proceeding through  $^{106}\text{Sb}$  [22]. Later, based on precise mass measurements [23], it was concluded that only 3% of the total flow proceeds through  $^{106}\text{Sb}$ , and that a stronger branch of 13% can be expected to proceed via  $^{107}\text{Sb}$ . In terms of proton separation energy,  $^{108}\text{Sb}$  is an even better candidate as a potential gateway nucleus, but this branch is suppressed by the long, 115 s [24],  $\beta$ -decay half-life of  $^{106}\text{Sn}$ . Furthermore, in another  $\alpha$ -decay study [18], it was shown that the Sn-Sb-Te cycle cannot proceed through  $^{105}\text{Sb}$ . However, it has been speculated [18,19] that it is possible for the cycle to flow via  $^{104}\text{Sb}$ , if this nucleus is more proton-bound than expected due to enhanced proton-neutron interactions [25], similarly to  $^{112}\text{Cs}$ .

To date, it is not certain whether the Sn-Sb-Te cycle proceeds through  $^{104}\text{Sb}$ . To address this question, the proton separation energy of  $^{104}\text{Sb}$  needs to be determined. Due to low production cross sections, precise mass measurements, as well as direct reaction rate studies, are beyond the reach of current experimental techniques. In addition, the expected proton decay branch of  $^{104}\text{Sb}$  is below 1% [26], which makes the direct observation of this proton decay difficult. However, as the  $Q_\alpha$  values of  $^{108}\text{I}$  and  $^{107}\text{Te}$  are known, this can be done indirectly by measuring the  $Q_p$  value of  $^{108}\text{I}$ , and using energy conservation [ $Q_p(^{104}\text{Sb}) = Q_\alpha(^{107}\text{Te}) + Q_p(^{108}\text{I}) - Q_\alpha(^{108}\text{I})$ ], see Fig. 1 for visualization. Multiple attempts to identify a proton emission branch in  $^{108}\text{I}$  have been undertaken [27–29], but without success. Here, we report the first observation of proton emission from  $^{108}\text{I}$ . From the measured  $Q_p(^{108}\text{I})$  value,  $Q_p(^{104}\text{Sb})$  is deduced. The implications for the termination of the  $rp$ -process are addressed. In addition, more precise properties of the  $^{108}\text{I}$ ,  $^{107}\text{Te}$ , and  $^{112}\text{Cs}$  nuclei are reported.

## 2. Experimental details

The neutron-deficient nuclei of interest were produced using the  $^{54}\text{Fe}(^{58}\text{Ni}, p3n)^{108}\text{I}$  fusion-evaporation reaction. The fusion-evaporation residues (referred to as recoils hereafter) were separated from the primary beam with the Fragment Mass Analyzer (FMA) [30]. The  $^{58}\text{Ni}$  beam, delivered by the ATLAS facility of Argonne National Laboratory, had an average intensity of 30 pA and an energy of 254 MeV. The total irradiation time of the self-supporting,  $450\text{-}\mu\text{g}/\text{cm}^2$  thick  $^{54}\text{Fe}$  targets was approximately 155 hours. The high beam intensity was accommodated by mounting the targets on a rotating wheel. A  $20\text{-}\mu\text{g}/\text{cm}^2$  thick stationary carbon charge-state reset foil was placed downstream from the target wheel. The FMA was set to collect recoils with  $A = 108$  and  $+26$  and  $+27$  charge states. Some  $^{107}\text{Te}$  and  $^{109}\text{I}$  recoils were collected as a side product due to partially overlapping mass-to-charge-state ratios, which were measured at the FMA focal plane with a position-sensitive parallel-grid avalanche counter (PGAC). After passing through PGAC, the recoils were implanted into a  $64\text{ mm} \times 64\text{ mm}$ ,  $100\text{-}\mu\text{m}$  thick,  $160 \times 160$  strip double-sided silicon strip detector (DSSD). The gain parameter of a linear energy calibration was obtained for the DSSD by using an  $\alpha$ -calibration source containing the  $^{240}\text{Pu}$  and  $^{244}\text{Cm}$  isotopes. The offset parameter was obtained separately for protons and  $\alpha$  particles from the observed activities of  $^{109}\text{I}$  ( $Q_p = 820(4)$  keV [31]) and  $^{108}\text{Te}$  ( $E_\alpha = 3314(4)$  keV [32]). The data from all channels were recorded independently, and each event was time-stamped with a 100 MHz clock. An approximately 4- $\mu\text{s}$  long waveform was collected for each DSSD event in order to analyze pile-up events.

The identification of the decay events of interest was based on the search for consecutive recoil implantation-decay ( $R$ - $d1$ ) or recoil implantation-decay-decay ( $R$ - $d1$ - $d2$ ) event chains in the same pixel of the DSSD. An event was considered as a recoil implantation if the PGAC yielded a horizontal position corresponding to mass number 108, the energy registered in the DSSD was greater than 15 MeV, and a time-of-flight condition between the PGAC and the DSSD was satisfied. An event without a PGAC signal was considered as a decay event, which may correspond to a proton decay, an  $\alpha$ -particle emission, or a  $\beta^+$  decay. Because the DSSD was rather thin,  $\beta^+$  particles were likely to punch through, resulting in a low-energy background.

## 3. Results

The energy spectrum of decay events for all observed  $R$ - $d1$  chains is displayed in Fig. 2. The energy deposited in the DSSD by  $\alpha$  decay of  $^{108}\text{I}$  and  $^{107}\text{Te}$ , once corrected for the  $\alpha$ -decay recoil effect [33,34], yielded respective  $Q_\alpha$  values of 4097(10) and 4007(10) keV. In Figs. 3(a) and 3(b), the time difference between the recoil and the decay event of  $R$ - $d1$  chains is shown for the  $\alpha$  decay of  $^{108}\text{I}$  and  $^{107}\text{Te}$ , respectively. The half-lives of 26.4(8) ms and 3.6(2) ms for  $^{108}\text{I}$  and  $^{107}\text{Te}$ , were obtained with the logarithmic-time scale method of Ref. [35], modified for two or three components. The long-lived component, labeled as “Bgr” in Fig. 3, is a result of decay-like events, randomly correlated with a recoil event. The third component in Fig. 3(b) is needed to account for partially overlapping  $\alpha$ -particle energies of the nuclei of interest.

Fig. 4 contains the energy-energy matrix for the two consecutive decay events in the observed  $R$ - $d1$ - $d2$  event chains, where  $d1$  and  $d2$  decay times were limited to 130 ms and 18 ms, i.e., approximately 5 times the half-lives of  $^{108}\text{I}$  and  $^{107}\text{Te}$ , respectively. In Fig. 4, a group of eight events are temporally and spatially (same pixel of the DSSD) correlated with the known  $\alpha$ -decay of  $^{107}\text{Te}$ , implying proton emission from  $^{108}\text{I}$ . The time distribution of these

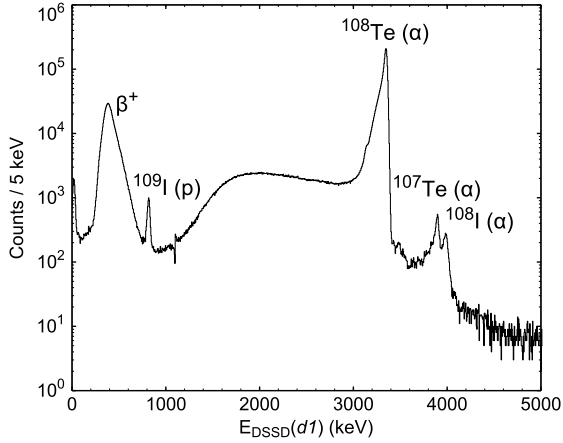


**Fig. 2.** Energy spectrum for all decay events observed as a member of a  $R$ - $d1$  event chain. The previously known activities are labeled. The discontinuity at the energy of 1100 keV is due to the different energy calibration for proton- and  $\alpha$ -decay events.

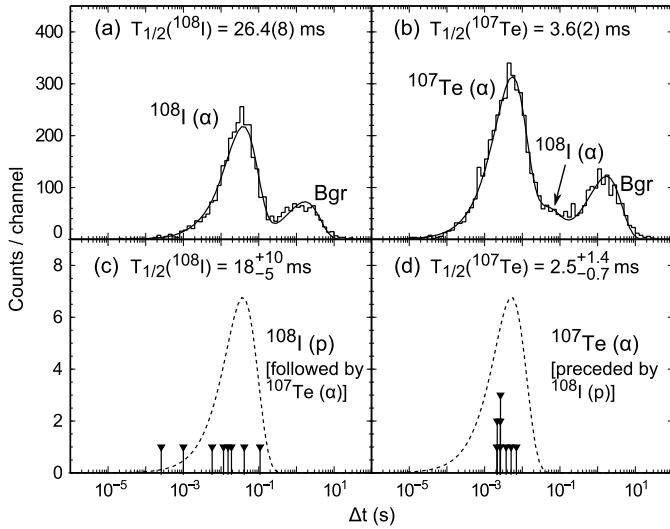


**Fig. 3.** Time difference between a recoil implantation and a subsequent decay event observed in the same pixel of the DSSD, when the decay is (a)  $^{108}\text{I}(\alpha)$ , (b)  $^{107}\text{Te}(\alpha)$  or (c)  $^{108}\text{I}(p)$  followed by the  $\alpha$  decay of  $^{108}\text{I}$ . In panel (d), the time difference between two subsequent decay events of  $^{108}\text{I}(p)$  and  $^{107}\text{Te}(\alpha)$  is presented. The quoted half-lives were obtained with the logarithmic time-scale method [35] (panels (a) and (b)) or maximum likelihood method [36] (panels (c) and (d)). The solid lines in (a) and (b) are fits to the data, and the dashed lines in (c) and (d) are the probability density distributions [35] corresponding to the half-lives obtained from these fits. The peak labeled “Bgr” corresponds to random correlations, see text for details.

eight proton-decay events is presented in Fig. 3(c), and for the subsequent  $\alpha$  decays, in Fig. 3(d). The half-lives of these decay chains, extracted with the maximum likelihood method [36], are similar to those obtained in Figs. 3(a) and 3(b), indicating proton and  $\alpha$ -particle emission from the same state of  $^{108}\text{I}$ . The energy peak corresponding to the  $^{108}\text{I}$  proton-decay events, seen in the inset of Fig. 4, corresponds to a proton-decay  $Q$  value of 597(13) keV. A proton-decay branch of  $b_p = 0.50(21)\%$  was deduced from the number of observed  $^{108}\text{I}$  proton and  $\alpha$  decays. The beta decay branch was also accounted for by comparing the present half-life of  $^{108}\text{I}$  and the theoretical partial  $\beta$ -decay half-life of 402 ms [37].

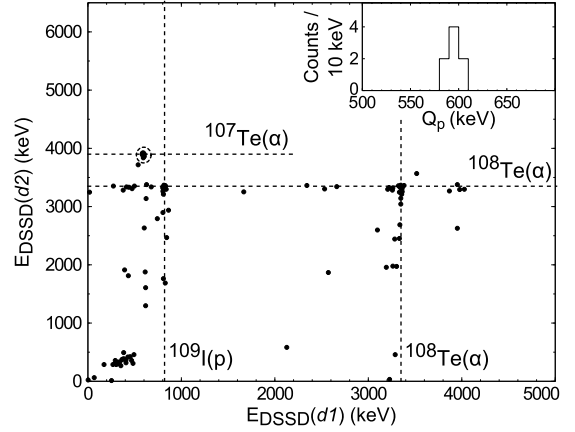


**Fig. 4.** Energy-energy correlation matrix for two subsequent decay events in  $R$ - $d1$ - $d2$  chains, when the  $R$ - $d1$  and  $d1$ - $d2$  time differences are less than 130 ms and 18 ms, respectively. The inset provides the energy spectrum of the newly observed  $^{108}\text{I}$  proton decay events, which are highlighted with a dashed circle in the main panel. Due to a high count rate in the DSSD and the long half-life,  $^{108}\text{Te}$   $\alpha$ -decay events self-correlate randomly. The dashed lines mark the energies of selected, previously identified, charged-particle decay activities in this region.

**Table 1**

$Q$  values, half-lives  $T_{1/2}$ , and mass excesses  $\Delta$  obtained in the present study compared to the literature values.

Quantity	This work	AME2016 [31,38,39]	Other studies
$Q_p(^{108}\text{I})$ (keV)	597(13)	600(110)	$\geq 240$ [19] $\leq 600$ [26]
$Q_p(^{104}\text{Sb})$ (keV)	510(20)	510(100)	$\geq 150$ [19] $\leq 520$ [19] $\leq 550$ [26]
$Q_\alpha(^{108}\text{I})$ (keV)	4097(10)	4100(50)	4099(5) [26]
$Q_\alpha(^{107}\text{Te})$ (keV)	4007(10)	4008(5)	3982(16) [40] 4012(10) [32]
$Q_\alpha(^{112}\text{Cs})$ (keV)	3940(20)	3930(120)	$\geq 3830$ [19] $\leq 4210$ [19] $\leq 3940$ [29]
$T_{1/2}(^{107}\text{Te})$ (ms)	3.6(2)	3.1(1)	$3.6_{-0.4}^{+0.6}$ [40] 3.1(1) [29]
$T_{1/2}(^{108}\text{I})$ (ms)	26.4(8)	36(6)	36(6) [29]
$\Delta(^{104}\text{Sb})$ (MeV)	-59.17(8)	-59.17(12)	
$\Delta(^{108}\text{I})$ (MeV)	-52.65(8)	-52.65(13)	

## 4. Discussion

The results obtained in this study are summarized in Table 1 and compared to those reported in the literature. These results are discussed in detail below.

### 4.1. Proton emission from $^{108}\text{I}$

The presently obtained  $Q_p$  value of 597(13) keV for  $^{108}\text{I}$  is in good agreement with the value of 600(110) keV reported in the recent mass evaluation of Ref. [31], as well as with an upper and lower limits of 600 [26] and 240 keV [19] set in earlier studies of  $^{108}\text{I}$ . Given the calculated deformation,  $\beta_2 = 0.15$  [41], and the odd-odd character of  $^{108}\text{I}$ , it is difficult to propose a firm configuration assignment for the proton decaying state. In the spherical shell model, the  $1d_{5/2}$  and  $2g_{7/2}$  orbitals are close to the Fermi surface for both protons and neutrons, indicating a high level density at low excitation energies. A WKB integral predicts partial proton-decay half-lives of approximately 150 ms or 70 s for a  $Q_p = 597$  keV proton emitted with an orbital angular momentum of  $l = 2$  or  $l = 4$ , respectively. A measured partial proton-decay half-life

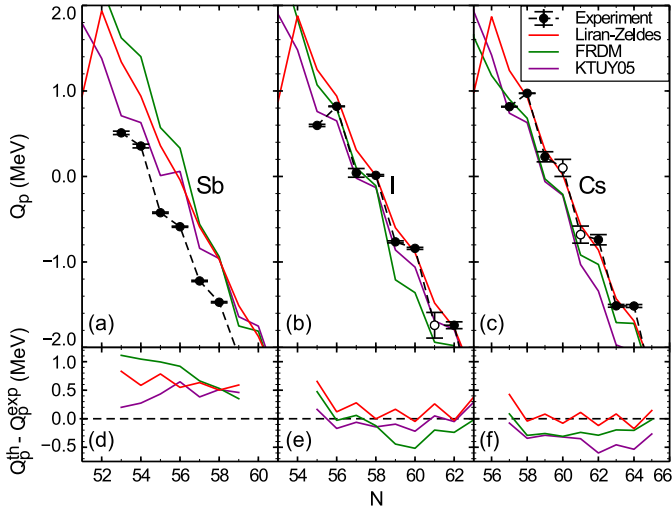


**Fig. 5.** Proton-emission  $Q$ -values of selected (a) Sb, (b) I, and (c) Cs isotopes. The data points marked with solid symbols are experimental values (this work and Refs. [18,23,31,39]), whereas interpolations from Ref. [31] are indicated with open symbols. The solid lines are predictions of different mass models (Liran-Zeldes [43], FRDM [41], and KTUY05 [44]), and the respective differences are shown in Panels (d)–(f).

of 5.3(22) s was deduced for  $^{108}\text{I}$  from the present half-life and branching ratio. The fact that the experimental value is between the two theoretical values, suggests that the proton is emitted with  $l=2$  from a state which is a strong admixture of  $1d_{5/2}$  and  $2g_{7/2}$  orbitals. For comparison, the WKB integral predicts a proton-decay half-life of approximately 10  $\mu\text{s}$  ( $l=2$ ) for  $^{109}\text{I}$ , whereas an experimental half-life of 93.5(3)  $\mu\text{s}$  [18] has been reported for this predominant proton emitter with a minuscule  $\alpha$ -decay branch.

The proton-decay half-life of neighboring  $^{109}\text{I}$  was calculated recently using the nonadiabatic quasiparticle approach as a function of deformation [17]. It was concluded that the experimental half-life is consistent with a deformation of  $\beta_2 \approx 0.15$  and asymmetry of  $\gamma \approx 15^\circ$ , and that the emission proceeds from a  $3/2^+$  state. This level was suggested to originate from a mixing of the  $\Omega^\pi = 1/2^+, 3/2^+$  Nilsson states, which are of  $2g_{7/2}$  and  $1d_{5/2}$  spherical parentage, respectively. It is expected that the deformation in  $^{108}\text{I}$  is similar to that of  $^{109}\text{I}$  [41]. However, in  $^{108}\text{I}$ , the odd proton has to be coupled to the odd neutron, similarly to the case of  $^{130}\text{Eu}$  [21]. The Gallagher-Moszkowski rule [42], applied to a proton and neutron occupying any combination of the  $1/2^+$  [431] or  $3/2^+$  [411] Nilsson orbitals, suggests a preferred coupling to a spin and parity of  $1^+$  or  $3^+$ . Since the  $^{107}\text{Te}$  ground state is expected to have a spin of  $5/2^+$ , the  $l=2$  proton emission from these orbitals is allowed, and would dominate over the  $l=4$  component. In order to quantitatively interpret proton emission from  $^{108}\text{I}$ , calculations using an approach similar to that of Ref. [17], but with the inclusion of the odd neutron [21], need to be performed.

#### 4.2. Proton-decay properties of $^{104}\text{Sb}$ , and their effect on the astrophysical $rp$ -process

Using the newly measured  $Q_p(^{108}\text{I}) = 597(13)$  keV and  $Q_\alpha(^{108}\text{I}) = 4097(10)$  keV values, together with the adopted  $Q_\alpha(^{107}\text{Te}) = 4008(5)$  keV [31], one can deduce a value of  $Q_p(^{104}\text{Sb}) = 510(20)$  keV. This is to be compared with the  $Q_p(^{104}\text{Sb}) = 510(100)$  keV, reported in the recent mass evaluation of Ref. [31], and a range of 150–520 keV estimated in Ref. [19]. A more precise value of  $-59.17(8)$  MeV for the mass excess  $\Delta$  of  $^{104}\text{Sb}$  can be obtained by using the present  $Q_p(^{104}\text{Sb})$  value and  $\Delta(^{103}\text{Sn})$  from Ref. [31]. In Fig. 5, the  $Q_p$  values obtained in this study are compared to

those of the nearby odd- $Z$  nuclei, as well as to the predictions of selected nuclear-mass models (Liran-Zeldes [43], FRDM [41], and KTUY05 [44]). Similarly to the  $^{112,113}\text{Cs}$  pair, the odd-odd  $^{108}\text{I}$  has a lower  $Q_p$  value than the less exotic, odd-even neighbor  $^{109}\text{I}$ . This is most likely due to the residual proton-neutron interactions between the odd proton and neutron [25]. In contrast,  $Q_p$  for odd-odd  $^{104}\text{Sb}$  is higher than that of  $^{105}\text{Sb}$ , possibly due to fewer proton-neutron pairs than in the iodine and cesium nuclei. It is noteworthy that none of the mass models predicts this  $Q_p$  decrease for the  $^{112,113}\text{Cs}$  and  $^{108,109}\text{I}$  pairs. Only the semiempirical shell-model formula of Liran and Zeldes [43] anticipates such a behavior, but not until at the  $N = Z$  line. All nuclear mass models appear to systematically overestimate the  $Q_p$  of antimony isotopes, but perform better for iodine and cesium nuclei. Liran-Zeldes model fits the data best on average, but it deviates for  $^{108}\text{I}$  and  $^{112}\text{Cs}$ . The KTUY05 model [44] performs the best for nuclei beyond the proton dripline. A pico-second scale ( $l=2$ ) or nano-second scale ( $l=4$ ) half-life is expected due to high  $Q_p$  value for the thus far unknown proton emitting isotopes of  $^{103}\text{Sb}$ ,  $^{107}\text{I}$ , and  $^{111}\text{Cs}$ . Given that a typical time-of-flight through a recoil separator is 1  $\mu\text{s}$ , the observation of these isotopes will be very difficult.

The Sn-Sb-Te cycle branching (see Fig. 4 in Ref. [18]), obtained using network calculations with a one-zone X-ray burst model [22], indicate clearly that, with the present  $Q_p(^{104}\text{Sb})$  value, there is no significant branching into the cycle via  $^{104}\text{Sb}$ . Hence, the discussion in Ref. [23] about the termination and final composition of the burst ashes of the astrophysical  $rp$ -process remains intact. However, these conclusions rely on the assumption that excited states do not play a role in the extraction of  $Q_p(^{104}\text{Sb})$ . Based on the present half-life analysis (see Fig. 3) protons and  $\alpha$  particles are emitted from the same state of  $^{108}\text{I}$ . Furthermore, the  $^{107}\text{Te}$   $\alpha$ -decay fine structure was characterized in Ref. [45], and the  $Q_\alpha(^{107}\text{Te}) = 4008(5)$  keV corresponds to a ground state-to-ground state  $\alpha$  decay. Therefore, the only scenario that cannot be excluded here, and that would decrease the present  $Q_p(^{104}\text{Sb})$ , is if the  $^{108}\text{I}$   $\alpha$  decay leads to an excited state of  $^{104}\text{Sb}$ . Such an excited state should have an energy greater than 1 MeV in order to allow a considerable branching into the Sn-Sb-Te cycle, which is unlikely. On the other hand, even a small change in  $Q_p(^{104}\text{Sb})$  would have an impact on the proton-decay branch of  $^{104}\text{Sb}$ . Assuming a proton emission from the spherical  $1d_{5/2}$  orbital and the present  $Q_p(^{104}\text{Sb})$  value, a WKB approximation predicts a partial proton-decay half-life of approximately 4 s for  $^{104}\text{Sb}$ . By comparing this to the measured half-life of  $^{104}\text{Sb}$  ( $440^{+150}_{-110}$  ms [46]), a proton-decay branch of approximately 10% can be expected. However, proton decay events following the  $\alpha$  decay of  $^{108}\text{I}$  were not observed in the present experiment, limiting the proton-decay branch to  $\lesssim 0.3\%$  for  $^{104}\text{Sb}$ , in fair agreement with the limit of  $\lesssim 1\%$  reported in Ref. [26]. This could occur if the  $2g_{7/2}$  proton orbital dominates the wave function of the  $^{104}\text{Sb}$  ground state, or if the spin of the ground state is greater than  $5\hbar$ , which would result in forbidden  $l=2$  proton emission. The predicted deformation of  $^{104}\text{Sb}$  is relatively small,  $\beta_2 = 0.075$  [41], but it might also slow down the proton emission from  $^{104}\text{Sb}$ .

#### 4.3. Properties of $^{107}\text{Te}$ , $^{108}\text{I}$ , and $^{112}\text{Cs}$ nuclei

The present  $Q_\alpha$  values for  $^{107}\text{Te}$  and  $^{108}\text{I}$  are in good agreement with those adopted in Ref. [31] and, together with the above improved mass excess of  $^{104}\text{Sb}$ , yield an improved value of  $\Delta(^{108}\text{I}) = -52.65(8)$  MeV, see Table 1 for comparison with the recommended values. The present half-life of  $T_{1/2}(^{107}\text{Te}) = 3.6(2)$  ms is slightly longer compared to the value of 3.1(1) ms, adopted in the recent nuclear data evaluation [38]. The latter value is identical to that given in Ref. [29], but an earlier study [40] reported

a half-life of  $3.6_{-0.4}^{+0.6}$  ms, in better agreement with the present data. The previously reported half-life of 36(6) ms [29] for  $^{108}\text{I}$  is marginally longer than that of 26.4(8) ms obtained here, but the total number of observed  $^{108}\text{I}$   $\alpha$  decays in the present study is approximately 30 times larger.

Similarly to the  $Q_p(^{104}\text{Sb})$ , also the  $Q_\alpha(^{112}\text{Cs})$  can be calculated via energy conservation as shown in Fig. 1. With the present  $Q_p(^{108}\text{I})$  value, and with  $Q_\alpha(^{111}\text{Xe}) = 3723.5(100)$  keV [32,39] and  $Q_p(^{112}\text{Cs}) = 816(4)$  keV [39], one calculates  $Q_\alpha(^{112}\text{Cs}) = 3940(20)$  keV, which is at the upper limit of 3940 keV obtained in Ref. [29]. It is more precise than the adopted value of 3930(120) keV [31], and the range of 3830–4210 keV proposed in Ref. [19]. In the latter study, an upper limit of 0.26% was obtained for the  $^{112}\text{Cs}$   $\alpha$ -decay branch. The present  $Q_\alpha(^{112}\text{Cs})$  value suggests a smaller  $\alpha$ -decay branch of  $0.07_{-0.04}^{+0.09}\%$  ( $l=0$ ) or  $0.03_{-0.02}^{+0.04}\%$  ( $l=2$ ), and this possibly explains why the  $\alpha$  decay of  $^{112}\text{Cs}$  was not observed in Ref. [19]. These branches were calculated with the method of Rasmussen [47], using the reduced  $\alpha$ -decay width of  $^{114}\text{Cs}$  ( $\delta^2 = 72_{-28}^{+48}$  keV [19,40]), and a half-life of 506(55)  $\mu\text{s}$  [19] for  $^{112}\text{Cs}$ .

## 5. Summary

A weak proton emission branch in  $^{108}\text{I}$  was observed with a proton-decay width consistent with that of hindered  $l=2$  emission. In order to assign a specific configuration for the proton emitting state, nonadiabatic quasiparticle calculations, similar to those presented in Refs. [17,21], are needed. Using the measured  $Q_p(^{108}\text{I})$  value, the proton-decay  $Q$  value for  $^{104}\text{Sb}$  was extracted indirectly. With this value, the network calculations with a one-zone X-ray burst model [18] predict no significant branching to the Sn-Sb-Te cycle via  $^{104}\text{Sb}$ . Because of the enhanced residual proton-neutron interactions in  $N \approx Z$  nuclei, the odd-odd  $^{108}\text{I}$  and  $^{112}\text{Cs}$  have a lower  $Q_p$  values than their less-exotic odd-even neighbors  $^{109}\text{I}$  and  $^{113}\text{Cs}$ , respectively. In contrast, the present  $Q_p(^{104}\text{Sb})$  is higher than that of  $^{105}\text{Sb}$ , possibly due to fewer proton-neutron pairs in the antimony isotopes.

## Acknowledgements

This material is based upon work supported by the U.S. Department of Energy, Office of Science, Office of Nuclear Physics, under Contracts No. DE-AC02-06CH11357 (ANL), No. DE-FG02-94ER40834 (UMCP), No. DE-FG02-94ER40848 (UMass Lowell), No. DE-FG02-97ER41041 (UNC), and No. DE-FG02-97ER41033 (TUNL). This research used resources of ANL's ATLAS facility, which is a DOE Office of Science User Facility. C.S. acknowledges that this work has been supported by the Academy of Finland under the Finnish Center of Excellence Programme (Contract No. 284612).

## References

- [1] T. Faestermann, M. Górska, H. Grawe, The structure of  $^{100}\text{Sn}$  and neighbouring nuclei, Prog. Part. Nucl. Phys. 69 (2013) 85, <https://doi.org/10.1016/j.pnpnp.2012.10.002>.
- [2] C.B. Hinke, M. Böhmer, P. Boutachkov, T. Faestermann, H. Geissel, et al., Superallowed Gamow-Teller decay of the doubly magic nucleus  $^{100}\text{Sn}$ , Nature 486 (2012) 341, <https://doi.org/10.1038/nature11116>.
- [3] R.D. Macfarlane, A. Siivola, New region of alpha radioactivity, Phys. Rev. Lett. 14 (1965) 114, <https://doi.org/10.1103/PhysRevLett.14.114>.
- [4] K. Auranen, D. Seweryniak, M. Albers, A.D. Ayangeakaa, S. Bottoni, et al., Superallowed  $\alpha$  decay to doubly magic  $^{100}\text{Sn}$ , Phys. Rev. Lett. 121 (2018) 182501, <https://doi.org/10.1103/PhysRevLett.121.182501>.
- [5] D. Seweryniak, K. Starosta, C.N. Davids, S. Gros, A.A. Hecht, et al.,  $\alpha$  decay of  $^{105}\text{Te}$ , Phys. Rev. C 73 (2006) 061301, <https://doi.org/10.1103/PhysRevC.73.061301>.
- [6] S.N. Liddick, R. Grzywacz, C. Mazzocchi, R.D. Page, K.P. Rykaczewski, et al., Discovery of  $^{109}\text{Xe}$  and  $^{105}\text{Te}$ : superallowed  $\alpha$  decay near doubly magic  $^{100}\text{Sn}$ , Phys. Rev. Lett. 97 (2006) 082501, <https://doi.org/10.1103/PhysRevLett.97.082501>.
- [7] Z. Janas, C. Mazzocchi, L. Batist, A. Blazhev, M. Górska, et al., Measurements of  $^{110}\text{Xe}$  and  $^{106}\text{Te}$  decay half-lives, Eur. Phys. J. A 23 (2005) 197, <https://doi.org/10.1140/epja/i2004-10076-x>.
- [8] L. Capponi, J.F. Smith, P. Ruotsalainen, C. Scholey, P. Rahkila, et al., Direct observation of the  $^{114}\text{Ba} \rightarrow ^{110}\text{Xe} \rightarrow ^{106}\text{Te} \rightarrow ^{102}\text{Sn}$  triple  $\alpha$ -decay chain using position and time correlations, Phys. Rev. C 94 (2016) 024314, <https://doi.org/10.1103/PhysRevC.94.024314>.
- [9] A. Florescu, A. Insolia, Microscopic calculation for  $\alpha$  and heavier cluster emissions from proton rich Ba and Ce isotopes, Phys. Rev. C 52 (1995) 726, <https://doi.org/10.1103/PhysRevC.52.726>.
- [10] S. Kumar, R.K. Gupta, Measurable decay modes of barium isotopes via exotic cluster emissions, Phys. Rev. C 49 (1994) 1922, <https://doi.org/10.1103/PhysRevC.49.1922>.
- [11] S. Kumar, D. Bir, R.K. Gupta,  $^{100}\text{Sn}$ -daughter  $\alpha$ -nuclei cluster decays of some neutron-deficient Xe to Gd parents: Sn radioactivity, Phys. Rev. C 51 (1995) 1762, <https://doi.org/10.1103/PhysRevC.51.1762>.
- [12] J. Dobaczewski, W. Nazarewicz, Limits of proton stability near  $^{100}\text{Sn}$ , Phys. Rev. C 51 (1995) R1070, <https://doi.org/10.1103/PhysRevC.51.R1070>.
- [13] E. Olsen, M. Pfützner, N. Birge, M. Brown, W. Nazarewicz, et al., Landscape of two-proton radioactivity, Phys. Rev. Lett. 110 (2013) 222501, <https://doi.org/10.1103/PhysRevLett.110.222501>.
- [14] E. Olsen, M. Pfützner, N. Birge, M. Brown, W. Nazarewicz, et al., Erratum: landscape of two-proton radioactivity [Phys. Rev. Lett. 110, 222501 (2013)], Phys. Rev. Lett. 111 (2013) 139903, <https://doi.org/10.1103/PhysRevLett.111.139903>.
- [15] V. Bugrov, S. Kadenskii, Proton decay of deformed nuclei, Yad. Fiz. 49 (1989) 1562.
- [16] V. Bugrov, S. Kadenskii, Proton decay of deformed nuclei, Sov. J. Nucl. Phys. 49 (1989) 967.
- [17] S. Modi, M. Patial, P. Arumugam, E. Maglione, L.S. Ferreira, Triaxiality in the proton emitter  $^{109}\text{I}$ , Phys. Rev. C 95 (2017) 054323, <https://doi.org/10.1103/PhysRevC.95.054323>.
- [18] C. Mazzocchi, R. Grzywacz, S.N. Liddick, K.P. Rykaczewski, H. Schatz, et al.,  $\alpha$  decay of  $^{109}\text{I}$  and its implications for the proton decay of  $^{105}\text{Sb}$  and the astrophysical rapid proton-capture process, Phys. Rev. Lett. 98 (2007) 212501, <https://doi.org/10.1103/PhysRevLett.98.212501>.
- [19] L. Cartegni, C. Mazzocchi, R. Grzywacz, I.G. Darby, S.N. Liddick, et al., Experimental study of the decays of  $^{112}\text{Cs}$  and  $^{111}\text{Xe}$ , Phys. Rev. C 85 (2012) 014312, <https://doi.org/10.1103/PhysRevC.85.014312>.
- [20] H. Suzuki, L. Sinclair, P.-A. Söderström, G. Lorusso, P. Davies, et al., Discovery of  $^{72}\text{Rb}$ : a nuclear sandbank beyond the proton drip line, Phys. Rev. Lett. 119 (2017) 192503, <https://doi.org/10.1103/PhysRevLett.119.192503>.
- [21] M. Patial, P. Arumugam, A.K. Jain, E. Maglione, L.S. Ferreira, Nonadiabatic quasiparticle approach for deformed odd-odd nuclei and the proton emitter  $^{130}\text{Eu}$ , Phys. Rev. C 88 (2013) 054302, <https://doi.org/10.1103/PhysRevC.88.054302>.
- [22] H. Schatz, A. Aprahamian, V. Barnard, L. Bildsten, A. Cumming, et al., End point of the  $rp$  process on accreting neutron stars, Phys. Rev. Lett. 86 (2001) 3471, <https://doi.org/10.1103/PhysRevLett.86.3471>.
- [23] V.V. Elomaa, G.K. Vorobjev, A. Kankainen, L. Batist, S. Eliseev, et al., Quenching of the SnSbTe cycle in the  $rp$  process, Phys. Rev. Lett. 102 (2009) 252501, <https://doi.org/10.1103/PhysRevLett.102.252501>.
- [24] R. Barden, R. Kirchner, O. Klepper, A. Plochocki, G.E. Rathke, et al., The Gamow-Teller beta decay of neutron-deficient even isotopes of tin, Z. Phys. A, At. Nucl. 329 (1988) 319, <https://doi.org/10.1007/BF01290237>.
- [25] P.J. Woods, C.N. Davids, Nuclei beyond the proton drip-line, Annu. Rev. Nucl. Part. Sci. 47 (1997) 541, <https://doi.org/10.1146/annurev.nucl.47.1.541>.
- [26] R.D. Page, P.J. Woods, R.A. Cunningham, T. Davinson, N.J. Davis, et al., Decays of odd-odd  $N - Z = 2$  nuclei above  $^{100}\text{Sn}$ : the observation of proton radioactivity from  $^{112}\text{Cs}$ , Phys. Rev. Lett. 72 (1994) 1798, <https://doi.org/10.1103/PhysRevLett.72.1798>.
- [27] A. Gillitzer, T. Faestermann, K. Hartel, P. Kienle, E. Nolte, Groundstate proton radioactivity of nuclei in the tin region, Z. Phys. A, At. Nucl. 326 (1987) 107, <https://doi.org/10.1007/BF01294577>.
- [28] R.D. Page, P.J. Woods, S.J. Bennett, M. Freer, B.R. Fulton, et al., Evidence for the alpha decay of  $^{108}\text{I}$ , Z. Phys. A, Hadrons Nucl. 338 (1991) 295, <https://doi.org/10.1007/BF01288193>.
- [29] R.D. Page, P.J. Woods, R.A. Cunningham, T. Davinson, N.J. Davis, et al., Alpha radioactivity above  $^{100}\text{Sn}$  including the decay of  $^{108}\text{I}$ , Phys. Rev. C 49 (1994) 3312, <https://doi.org/10.1103/PhysRevC.49.3312>.
- [30] C.N. Davids, J.D. Larson, The argonne fragment mass analyzer, Nucl. Instrum. Methods Phys. Res., Sect. B, Beam Interact. Mater. Atoms 40–41 (1989) 1224, [https://doi.org/10.1016/0168-583X\(89\)90624-1](https://doi.org/10.1016/0168-583X(89)90624-1).
- [31] M. Wang, G. Audi, F.G. Kondev, W.J. Huang, S. Naimi, et al., The AME2016 atomic mass evaluation (II). Tables, graphs and references, Chin. Phys. C 41 (2017) 030003, <http://stacks.iop.org/1674-1137/41/i=3/a=030003>.

- [32] F. Heine, T. Faestermann, A. Gillitzer, J. Homolka, M. Köpf, et al., Proton and alpha radioactivity of very neutron deficient Te, I, Xe and Cs isotopes, studied after electrostatic separation, *Z. Phys. A, Hadrons Nucl.* 340 (1991) 225, <https://doi.org/10.1007/BF01303837>.
- [33] S. Hofmann, S. Heinz, R. Mann, J. Maurer, J. Khuyagbaatar, et al., The reaction  $^{48}\text{Ca} + ^{248}\text{Cm} \rightarrow ^{296}116^*$  studied at the GSI-SHIP, *Eur. Phys. J. A* 48 (2012) 62, <https://doi.org/10.1140/epja/i2012-12062-1>.
- [34] S. Hofmann, G. Münzenberg, K. Valli, F.P. Heßberger, J.R.H. Schneider, et al., Stopping of Alpha-Recoil Atoms in Silicon, GSI Scientific Report 1981, 1982, p. 241, <http://repository.gsi.de/record/53550/files/GSI-Report-1982-1.pdf>.
- [35] K.H. Schmidt, A new test for random events of an exponential distribution, *Eur. Phys. J. A* 8 (2000) 141, <https://doi.org/10.1007/s100500070129>.
- [36] K.H. Schmidt, C.C. Sahm, K. Pielenz, H.G. Clerc, Some remarks on the error analysis in the case of poor statistics, *Z. Phys. A, At. Nucl.* 316 (1984) 19, <https://doi.org/10.1007/BF01415656>.
- [37] M. Hirsch, A. Staudt, K. Muto, H. Klapdorkleingrothaus, Microscopic predictions of  $\beta$ +/ $\text{EC}$ -decay half-lives, *At. Data Nucl. Data Tables* 53 (1993) 165, <https://doi.org/10.1006/adnd.1993.1004>.
- [38] G. Audi, F.G. Kondev, M. Wang, W.J. Huang, S. Naimi, The NUBASE2016 evaluation of nuclear properties, *Chin. Phys. C* 41 (2017) 030001, <http://stacks.iop.org/1674-1137/41/i=3/a=030001>.
- [39] W.J. Huang, G. Audi, M. Wang, F.G. Kondev, S. Naimi, et al., The AME2016 atomic mass evaluation (I). Evaluation of input data; and adjustment procedures, *Chin. Phys. C* 41 (2017) 030002, <http://stacks.iop.org/1674-1137/41/i=3/a=030002>.
- [40] D. Schardt, R. Kirchner, O. Klepper, W. Reisdorf, E. Roeckl, et al., Alpha decay studies of tellurium, iodine, xenon and cesium isotopes, *Nucl. Phys. A* 326 (1979) 65, [https://doi.org/10.1016/0375-9474\(79\)90367-1](https://doi.org/10.1016/0375-9474(79)90367-1).
- [41] P. Möller, A. Sierk, T. Ichikawa, H. Sagawa, Nuclear ground-state masses and deformations: FRDM(2012), *At. Data Nucl. Data Tables* 109–110 (2016) 1, <https://doi.org/10.1016/j.adt.2015.10.002>.
- [42] C.J. Gallagher, S.A. Moszkowski, Coupling of angular momenta in odd-odd nuclei, *Phys. Rev.* 111 (1958) 1282, <https://doi.org/10.1103/PhysRev.111.1282>.
- [43] S. Liran, N. Zeldes, A semiempirical shell-model formula, *At. Data Nucl. Data Tables* 17 (1976) 431, [https://doi.org/10.1016/0092-640X\(76\)90033-4](https://doi.org/10.1016/0092-640X(76)90033-4).
- [44] H. Koura, T. Tachibana, M. Uno, M. Yamada, Nuclidic mass formula on a spherical basis with an improved even-odd term, *Prog. Theor. Phys.* 113 (2005) 305, <https://doi.org/10.1143/PTP.113.305>.
- [45] D. Seweryniak, W.B. Walters, A. Woehr, M. Lipoglavsek, J. Shergur, et al., Population of the 168-keV ( $g_{7/2}$ ) excited state in  $^{103}\text{Sn}$  in the  $\alpha$  decay of  $^{107}\text{Te}$ , *Phys. Rev. C* 66 (2002) 051307, <https://doi.org/10.1103/PhysRevC.66.051307>.
- [46] T. Faestermann, J. Friese, H. Geissel, R. Gernhäuser, H. Gilg, et al., Decay Properties of  $^{100}\text{Sn}$  and Neighbouring Nuclei, GSI Scientific Report 1996-1, 1996, p. 21, <http://repository.gsi.de/record/53536>.
- [47] J.O. Rasmussen, Alpha-decay barrier penetrabilities with an exponential nuclear potential: even-even nuclei, *Phys. Rev.* 113 (1959) 1593, <https://doi.org/10.1103/PhysRev.113.1593>.